Macromolecules

Article

pubs.acs.org/Macromolecules

# Synthesis of Functional Polypropylene Containing Hindered Phenol Stabilizers and Applications in Metallized Polymer Film Capacitors

Gang Zhang, Houxiang Li, Martin Antensteiner, and T. C. Mike Chung*

Department of Materials Science and Engineering, The Pennsylvania State University, University Park, Pennsylvania 16802, United States

Supporting Information

**ABSTRACT:** This paper discusses a new family of polymeric stabilizers (antioxidants) containing a polypropylene backbone and several pendant hindered phenol groups (PP-HP), with both random and tapered copolymer microstructures. They are effectively prepared by Steglich esterification of the corresponding hydroxylated polypropylene (PP-OH) copolymers with the hindered phenol molecule containing a carboxylic acid moiety. Some resulting PP-HP copolymers show significantly higher thermal-oxidative stability than the pristine PP polymer and the commercial PP products that contain a small amount of organic hindered phenol stabilizers. The better oxidative stability was also observed in PP/PP-HP blends under elevated temperatures. Overall, the PP chain degradation temperature increases with the increase of HP concentration in the matrix. The effectiveness of the PP-HP stabilizer is attributed to its comparability and cocrystallization with the PP homopolymer, which result in a uniform distribution of hindered phenol moieties. It also allows the relatively higher concentration of hindered phenol (polar) moieties in the PP (nonpolar) matrix without phase separation. In addition to the known advantages of polymer-bonded stabilizers, with low mobility and volatility to prevent loss through diffusion and/or extraction (particularly acute in films and coatings), the PP-HP thin dielectric films with uniform morphology show a higher dielectric constant and maintain low dielectric loss, particularly for the tapered PP-HP copolymers with high crystallinity.

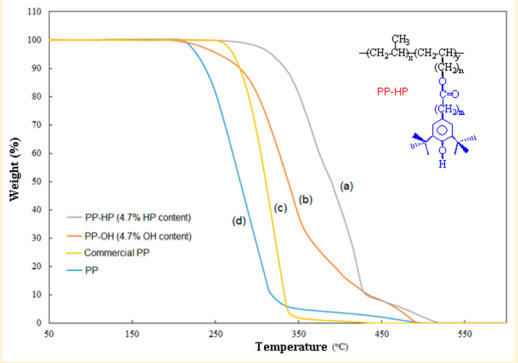


## INTRODUCTION

It is a common practice in the polyolefin industry to incorporate a small amount of stabilizers (antioxidants)[1−6] into the polymer material right after the polymerization to inhibit its oxidation reaction during melt processes at high temperature and outdoor applications under long-term UV exposure and heat. Polypropylene (PP) in its pristine state (without stabilizer) is inherently unstable due to the existence of a labile tertiary proton in each monomer unit.[7−10] In the presence of heat, light, and reactive metals (catalyst residues), the tertiary proton is subjected to oxygen oxidation then chain degradation, as illustrated in Scheme 1.

The degradation of the polymer chain follows an autoxidation and catalytic mechanism.[11] The polymer radical (**I**) is formed after removing a tertiary proton by heat or UV radiation, which spontaneously reacts with an oxygen molecule to form the peroxy radical (**II**). The peroxy radical then removes another tertiary proton (R−H) from another polymer chain to form a hydroperoxide (C−O−O−H) intermediate (**III**) that is decomposed under heat. Two possible decomposition pathways, cleaving either O−O or C−O bonds in the C−O−O−H moiety, lead to the spontaneous PP chain degradation to form PP with a terminal aldehyde group (**IV**) or PP with a terminal olefinic group (**VI**), respectively. On the other hand, the newly formed polymer radicals (**V**) and (**VII**) continue proton extraction and autoxidation−degradation cycle unless countermeasures are taken to halt the reaction process.

Stabilizers (antioxidants) are usually present in commercial polyolefins (i.e., PE and PP). The most common stabilizers include octadecyl-3-(3,5-di-*tert*-butyl-4-hydroxyphenyl)-propionate (IRGANOX1076) and pentaerythritol tetrakis(3-(3,5-di-*tert*-butyl-4-hydroxyphenyl)propionate) (IRGANOX1010),[12,13] as illustrated in Scheme 2. They contain single or multiple hindered phenol moieties, with facile hydrogen-donating activity, to compete with polymer protons (R−H) for peroxy radicals (**II**) and alkyl radicals (**V** and **VII**), thus inhibiting the oxidation−degradation cycles.[14] A low concentration (<1 wt %) of hindered phenol stabilizer existing in the polymer matrix can prevent or retard polymer chain degradation during polymer processes and applications. However, there are several concerns that often severely limit the effectiveness of the stabilizer and the product's long-term performance. The poor solubility of the polar stabilizer molecules in the semicrystalline nonpolar PE and PP matrix can lead to some problems, including inhomogeneous

**Received:** March 2, 2015
**Revised:** April 15, 2015
**Published:** April 24, 2015





DOI: 10.1021/acs.macromol.5b00439
*Macromolecules* 2015, 48, 2925−2934

Scheme 1

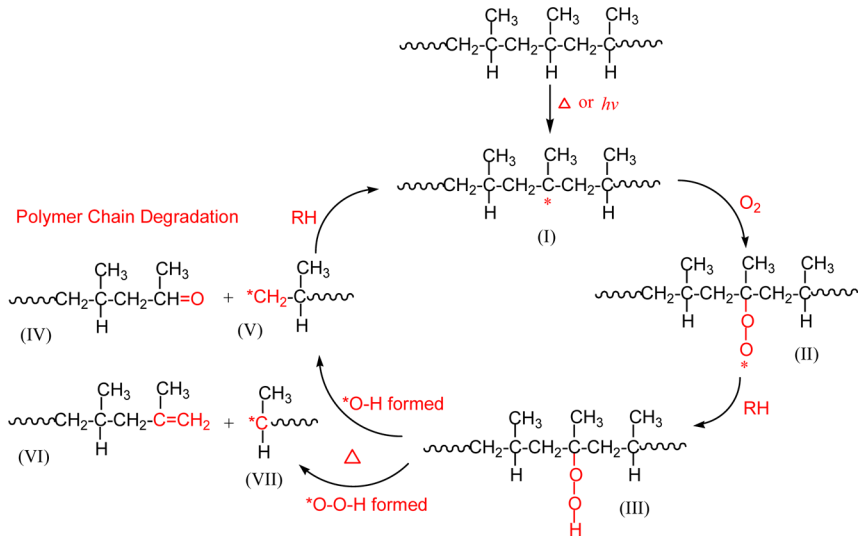


Scheme 2

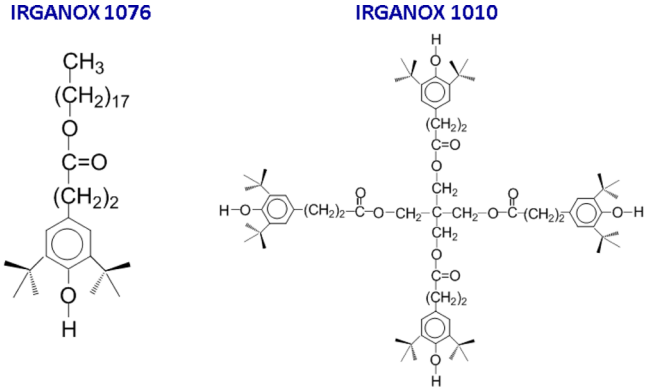


distribution of the stabilizer with less than minimum effective concentration, stabilizer migration to surfaces, and accelerated stabilizer loss when exposed to solvents, heat, or strong electric fields.[15,16] There have been research efforts to develop polymeric (polymer-bonded) stabilizers with reduce mobility and volatility to improve the long-term stability of polymer products.[17−20] This approach is particularly acute in thin film and coating applications. However, there are only few reports by Dr. Wilén et al. discussing polyolefin-bonded stabilizers[21−23] prepared by metallocene-mediated copolymerization of $\alpha$-olefin and antioxidant comonomers. Most synthesis strategies are based on free-radical mediated copolymerization and grafting reactions with monomers containing hindered phenol moieties.[24−29] Because of incompatibility and limited solubility, the resulting styrene- or acrylate-based polymeric stabilizers usually show limited effectiveness. On the other hand, the free radical grafting reactions on PE and PP polymers are known to be accompanied by many side reactions,[30] including the chain degradation shown in Scheme 1, low yield, byproducts, and colored material.

In the dielectric applications, the presence of impurities (polar molecules) or multiple phases with different dielectric domains in the dielectric films are oftentimes highly undesirable with major concerns.[31] Under high applied electric fields, the diffusion of polar molecules and inhomogeneous field distribution at the interfaces cause dielectric loss, and the generated heat deforms thin films and results in early breakdown. Current state-of-the-art metalized polymer film capacitors are based on biaxial oriented polypropylene (BOPP) thin films (thickness ~10 $\mu$m) that commonly contain less than 1 wt % of the IRGANOX1010 stabilizer.[32,33] Despite its high dielectric strength (breakdown electric field >700 MV/m), the BOPP capacitors are usually operated at the field <400 MV/m. Combined with a low dielectric constant ($\varepsilon$ = 2.2), BOPP-based thin film capacitors can only provide consistent energy density in the range of 1−2 J/cm$^3$.[34−36] It is scientifically interesting to explore how it is possible to increase its dielectric activities ($\varepsilon$ value), long-term (oxidative and thermal) stability, and breakdown strength ($E$) in order to achieve higher energy density in PP-based capacitors. These past few years, our group has been investigating several functional PP polymers with the objective of understanding the structure−property relationship and increasing PP energy density.[37−44] In this paper, we will discuss a new approach to incorporate hindered phenol antioxidant groups in the PP polymer chain, which may not only increase the thermal-oxidative stability but also offer higher dielectric responses in PP dielectrics.

## EXPERIMENTAL SECTION

**Materials and Instrumentation.** All $O_2$- and moisture-sensitive manipulations were carried out inside an argon-filled Vacuum Atmosphere drybox. *rac*-$Me_2Si$[2-Me-4-Ph(Ind)]$_2ZrCl_2$ catalyst was prepared using the published procedures.[45] $TiCl_3$·AA, $AlEt_2Cl$, MAO (10 wt % in toluene), 10-undecen-1-ol, chlorotrimethylsilane, triethylamine, calcium hydride (Sigma-Aldrich), 1-(3-(dimethylamino)propyl)-3-ethylcarbodiimide and 4-*N*,*N*-dimethylaminopyridine (VWR Scientific), octadecyl-3-(3,5-di-*tert*-butyl-4-hydroxyphenyl)-propionate, pentaerythritol tetrakis(3-(3,5-di-*tert*-butyl-4-hydroxyphenyl)propionate), 3,5-bis(*tert*-butyl)-4-hydroxybenzoic acid, 3,5-bis(*tert*-butyl)-4-hydroxyphenylpropionic acid (BASF), and propylene (Matheson Gas) were used as received. Toluene (Wiley Organics) was distilled over sodium benzophenone under argon.

All high temperature $^1$H NMR spectra were recorded on a Bruker AM-300 spectrometer, with the polymer samples dissolved in 1,1,2,2-tetrachloroethane-$d_2$ at 110 °C. The thermal transition data were obtained with a TA Instruments Q100 differential scanning calorimeter (DSC) at a heating rate of 20 °C/min. Thermogravimetric (TGA) analysis was performed from a range of 20−700 °C at a 10 °C/min rate. The molecular weights of the polymers were determined by intrinsic viscosity of polymer measured in decahydronaphthalene


DOI: 10.1021/acs.macromol.5b00439
*Macromolecules* 2015, 48, 2925−2934

Scheme 3

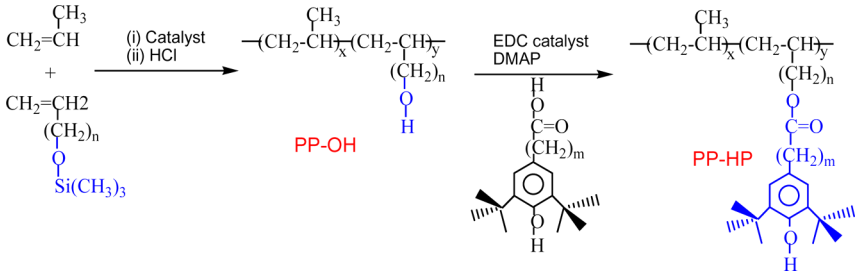


(decalin) dilute solution at 135 °C with a Cannon-Ubbelohde viscometer. The viscosity molecular weight was calculated by the Mark–Houwink equation: $[\eta] = KM_v^{\alpha}$ where $K = 1.05 \times 10^{-5}$ and $\alpha = 0.80$.[46] For the dielectric constant and D-E polarization–depolarization cycle measurements, gold electrodes (thickness ~50 nm) were sputtered on both surfaces of the polymer film. The electric displacement–electric field was measured by a modified Sawyer–Tower circuit and a linear variable differential transducer (LVDT), driven by a lock-in amplifier (Stanford Research Systems, Model SR830). Electric fields ranging from 100 to 600 MV/m were applied across the polymer film using an amplified ramp waveform at 10 Hz.

**Synthesis of PP–OH Copolymers Using *rac*-$Me_2Si$[2-Me-4-Ph(Ind)]$_2ZrCl_2$/MAO Catalyst.** The OH group in 10-undecen-1-ol comonomer was protected by silane group before the polymerization step. In a 1 L flask, equipped with a magnetic stirrer, 34.46 g of 10-undecen-1-ol and 20.22 g of triethylamine were dissolved into 500 mL of THF, and then 21.72 g of chlorotrimethylsilane was slowly introduced at room temperature. The white powders appeared immediately. The suspension was stirred at 60 °C for 8 h, and the white powders were filtered and removed. The resulting yellow solution was distilled under vacuum, and the fraction at 60 °C was redistilled over $CaH_2$ before use.

In a typical polymerization reaction, a dried Parr 450 mL stainless autoclave equipped with a mechanical stirrer was charged with 75 mL of toluene, 5 mL of MAO (5 wt % in toluene), and 2.0 g of 10-undecen-1-oxytrimethylsilane after purging with propylene gas. About 5 μmol of *rac*-$Me_2Si$[2-Me-4-Ph(Ind)]$_2ZrCl_2$ in the toluene solution was then syringed into the rapidly stirring solution under propylene pressure to initiate the polymerization. After 20 min of reaction at 40 °C under 120 psi pressure of propylene gas, the polymer solution was quenched with methanol. The resulting product was washed with HCl/methanol (0.5 M), methanol, and THF two times each and then vacuum-dried at 60 °C. About 7.22 g of PP-OH copolymer was obtained with a catalytic activity of 4300 kg of polymer/(mol of Zr·h).

**Synthesis of PP-HP Copolymer by Esterification of PP-OH.** The esterification reaction of the PP-OH copolymer was carried out by mixing PP-OH with two carboxylic acid molecules that also contains a hindered phenol moiety, i.e., 3,5-bis(*tert*-butyl)-4-hydroxybenzoic acid and 3,5-bis(*tert*-butyl)-4-hydroxyphenylpropionic acid, in the presence of 1-(3-(dimethylamino)propyl)-3-ethylcarbodiimide (EDC) and 4-*N*,*N*-dimethylaminopyridine (DMAP). In a typical reaction run, under an argon atmosphere, 2 g of PP-OH copolymer with 2.31 mol % of OH content was mixed with 1.8 g of 3,5-bis(*tert*-butyl)-4-hydroxybenzoic acid, 0.22 g of DMAP, and 100 mL of toluene in a 500 mL round-bottom flask equipped with a stirrer and a condenser. After adding 1.37 g of the EDC reagent, the esterification reaction was carried out at 110 °C for 12 h. The resulting PP-HP copolymer was precipitated in 600 mL of methanol and then washed with methanol a few times before drying the polymer in a vacuum oven at 70 °C overnight.

## RESULTS AND DISCUSSION

This paper discusses a new class of polypropylene-based stabilizers (PP-HP copolymers) containing a PP backbone and various concentrations of hindered phenol (HP) moieties located in the pendant side chains. Both random and tapered

**Table 1. Summary of Two Sets of PP-HP Copolymers with Taped and Random Microstructures**

| polymer[a] | [HP][b] (mol %) | $M_v$[c] (×10$^{-3}$ g/mol) | $T_m$[d] (°C) | $\Delta H$[d] (J/g) | $T_c$[d] (°C) |
|---|---|---|---|---|---|
| A-PP-HP-1 | 0.8 | 620 | 157 | 66 | 110 |
| A-PP-HP-2 | 1.7 | 388 | 157 | 53 | 101 |
| A-PP-HP-3 | 3.2 | 311 | 157 | 48 | 104 |
| A-PP-HP-4 | 4.2 | 372 | 158 | 46 | 107 |
| B-PP-HP-1 | 1.5 | 446 | 143 | 86 | 107 |
| B-PP-HP-2 | 3.5 | 314 | 116 | 27 | 67 |
| B-PP-HP-3 | 4.7 | 223 | 107 | 12 | 62 |
| B-PP-HP-4 | 6.0 | 181 | 82 | 6 | 55 |

[a]Set A: preparation of tapered PP-OH copolymers involves 0.200 g of $TiCl_3$·AA, 5 mL of $Al(Et)_2Cl$ (10 wt % in toluene), 75 mL of toluene, 30 psi propylene pressure, and a specific amount of 10-undecen-1-oxytrimethylsilane comonomers at 60 °C. Set B: preparation of random PP-OH copolymers involves 5 μmol of *rac*-$Me_2Si$[2-Me-4-Ph(Ind)]$_2ZrCl_2$ catalyst/5 mL of MAO (10 wt % in toluene), 75 mL of toluene, 120 psi propylene gas, and a specific amount of 10-undecen-1-oxytrimethylsilane comonomers at 40 °C. [b][HP] indicates the hindered phenol content (mol %) in the copolymers. [c]Estimated by intrinsic viscosity of polymer/decalin dilute solution at 135 °C with $K = 1.05 \times 10^{-4}$ dL/g and $\alpha = 0.8$. [d]Determined by DSC curves at a heating rate of 20 °C/min.

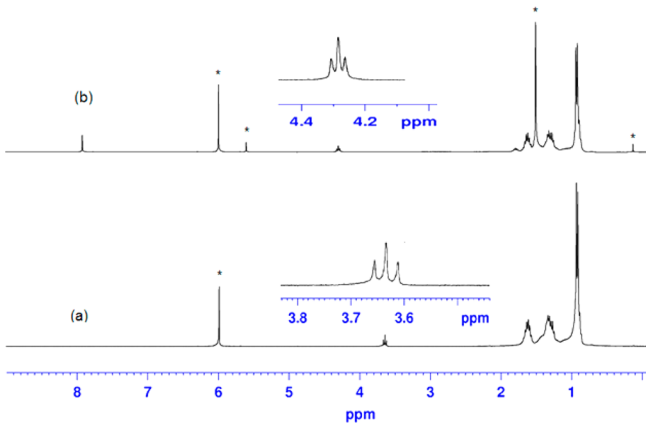


**Figure 1.** $^1$H NMR spectra of (a) PP-OH copolymer with 4.7 mol % OH content (B-PP-OH-3) and (b) the corresponding PP-HP copolymer.

PP-HP copolymer microstructures were synthesized and compared to understand their structure–property relationship, including their cocrystallization ability with PP homopolymer, thermal-oxidative stability, and dielectric properties. The objective is to identify the most suitable polymeric stabilizer (antioxidant) for PP dielectrics, which not only improves PP thermal and environmental stability during melt processes and



DOI: 10.1021/acs.macromol.5b00439
Macromolecules 2015, 48, 2925–2934

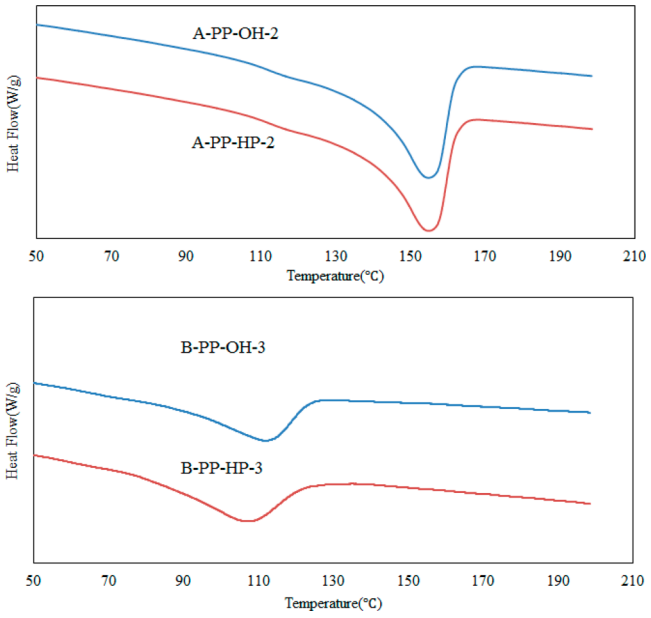


**Figure 2.** Comparison of DSC curves between PP-HP and the corresponding PP-OH copolymers (top) prepared by Ziegler–Natta catalyst and (bottom) prepared by metallocene catalyst.

long-term applications under high applied electric fields but also increases its dielectric performance.

**Polymer Synthesis.** Scheme 3 illustrates the synthesis route to prepare the PP-HP copolymers with well-controlled molecular structures and high yields. The reaction scheme involves two steps, including the propylene/undecenyloxytrimethylsilane copolymerization to prepare the hydroxyl-modified polypropylene (PP-OH) intermediate[47] and the subsequent Steglich esterification[48] of OH groups with the hindered phenol molecule containing a carboxylic acid group to form the PP-HP copolymer.

In our previous papers,[49−51] we have discussed two effective routes to prepare high PP-OH copolymers with "tapered" microstructures. The chemistry involves the copolymerization reactions of propylene/hexenyl-9-BBN (9-BBN: 9-borobicyclo-

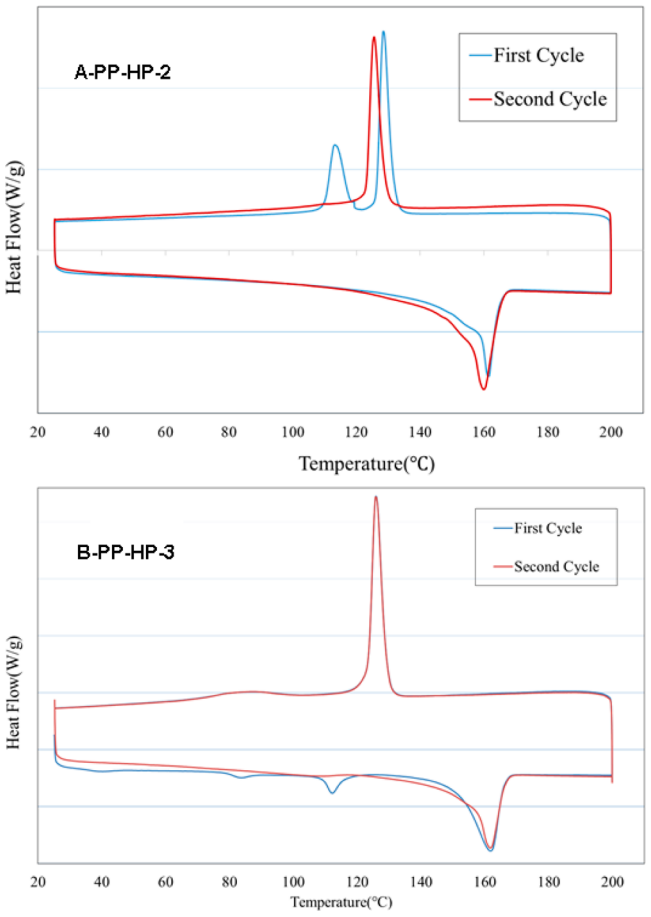


**Figure 4.** DSC curves of the PP/PP-HP (1/1) blend during the first and second heating–cooling cycles using (top) tapered A-PP-HP-2 copolymer and (bottom) random B-PP-HP-3 copolymer.

[3,3,1]nonane) or propylene/10-undecen-1-oxytrimethylsilane using heterogeneous Ziegler–Natta ($TiCl_3$·AA/$AlEt_2Cl$) catalyst. Both borane and silane functional groups in comonomers are stable in heterogeneous Ziegler–Natta catalyst, and the incorporated borane and silane pendant groups along the PP

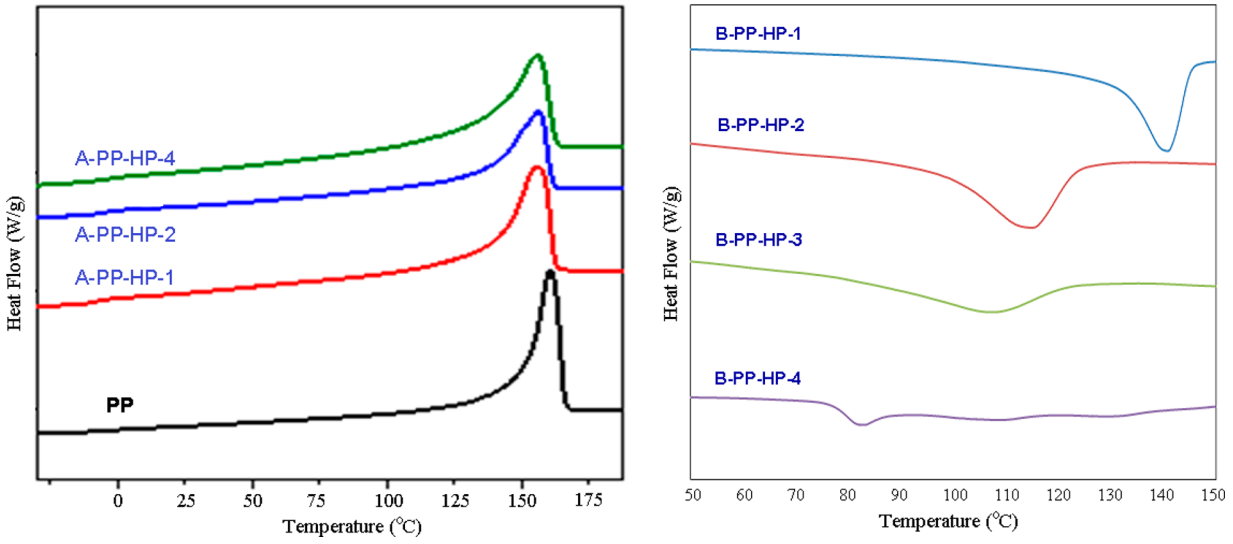


**Figure 3.** DSC curves of PP homopolymer and two sets of PP-HP copolymers summarized in Table 1 with (left) tapered and (right) random copolymer microstructures, respectively.



DOI: 10.1021/acs.macromol.5b00439
*Macromolecules* 2015, 48, 2925−2934

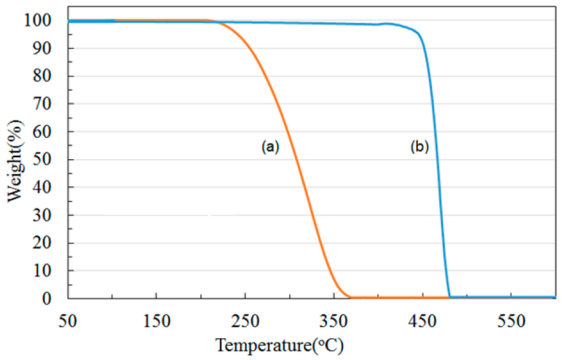


**Figure 5.** TGA curves of a pure PP homopolymer (a) in air and (b) under $N_2$ atmosphere.

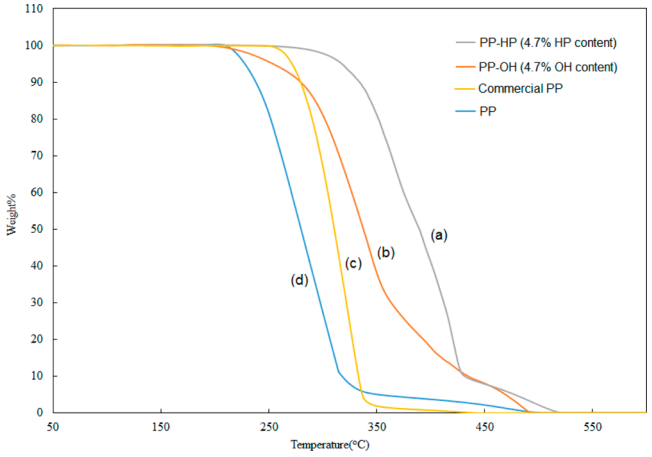


**Figure 6.** TGA curves of (a) PP-PH copolymer with 4.7 mol % HP content, (b) the corresponding PP-OH copolymer with 4.7 mol % OH content, (c) commercial PP with IRGANOX1010 stabilizer, and (d) pure PP polymer.

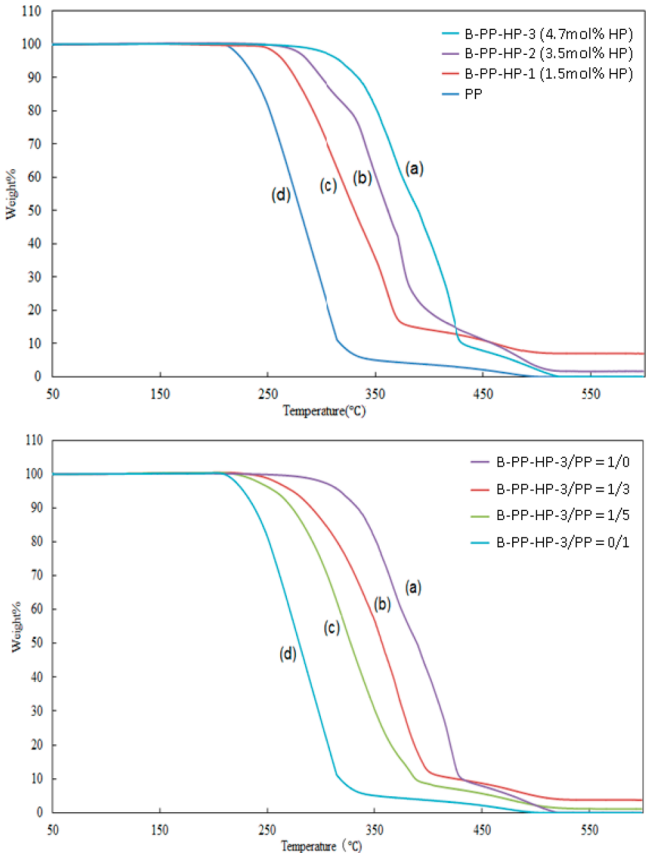


**Figure 7.** TGA curve comparison of (top) several random B-PP-HP copolymers with (a) 4.7, (b) 3.5, (c) 1.5, and (d) 0 HP contents and (bottom) B-PP-HP-3/PP blends with (a) 1/0, (b) 5/1, (c) 3/1, and (d) 0/1 weight ratios.

polymer chains can be completely interconverted to the corresponding OH groups during the sample work-up procedure. However, due to the large difference in reactivity ratios between propylene and both borane and silane bulky comonomers in the heterogeneous Ziegler–Natta polymerization, all resulting PP-OH copolymers show a "tapered" molecular structure with long propylene sequences and a broad composition distribution. In addition, the copolymer composition is broadened with the continuous change of comonomer feed ratio during the batch reaction. In this paper, we have extended the chemistry to employ a homogeneous isospecific *rac*-$Me_2Si[2\text{-}Me\text{-}4\text{-}Ph(Ind)]_2ZrCl_2$/MAO metallocene catalyst in the propylene/10-undecen-1-oxytrimethylsilane copolymerization, with the objective of preparing "random" PP-OH copolymers as well as narrow molecular weight and composition distributions.

Table 1 summarizes two sets of PP-HP copolymers with tapered and random microstructures. They are converted from the corresponding PP-OH copolymers prepared by propylene/10-undecen-1-oxytrimethylsilane copolymerization reactions using the heterogeneous Ziegler–Natta and homogeneous metallocene catalysts, respectively. The experimental details and results of both copolymerization reactions are shown in Table S1 of the Supporting Information. During the batch reaction, with a constant propylene pressure and reducing comonomer concentration, we limited the reaction time to 15–20 min for minimizing the change of comonomer feed ratio and the resulting copolymer composition. The reduction of comonomer concentration in each copolymerization reaction was controlled to <20% in Ziegler–Natta and <50% in metallocene cases, respectively. Overall, both heterogeneous Ziegler–Natta and homogeneous metallocene catalysts are effective in the preparation of PP-OH copolymers with high molecular weights, without any indication of a catalyst poisoning by the silane-protected OH group. However, the *rac*-$Me_2Si[2\text{-}Me\text{-}4\text{-}Ph(Ind)]_2ZrCl_2$/MAO catalyst exhibits much higher catalyst activity than the $TiCl_3$·AA/$AlEt_2Cl$ catalyst in forming PP-OH polymers with high OH content.

All PP-OH copolymers were successfully interconverted to the corresponding PP-HP copolymers by Steglich esterification reactions using two hindered phenol molecules that contain a carboxylic acid group, including 3,5-bis(*tert*-butyl)-4-hydroxybenzoic acid and 3,5-bis(*tert*-butyl)-4-hydroxyphenylpropionic acid, which have the same hindered phenol moiety shown in the commercial IRGANOX1076 and 1010 (Scheme 2). This esterification reactions were facilitated by 1-(3-(dimethylamino)propyl)-3-ethylcarbodiimide (EDC) and 4-*N*,*N*-dimethylaminopyridine (DMAP) under mild reaction conditions. Figures 1 compares the $^1$H NMR spectra of a typical pair of PP-OH with 4.7 mol % OH content and the resulting PP-HP copolymers, using 3,5-bis(*tert*-butyl)-4-hydroxybenzoic acid. Both spectra exhibit three major chemical shifts at 0.95, 1.35, and 1.65 ppm, corresponding to the methine, methylene, and methyl groups in polypropylene. The triplet


DOI: 10.1021/acs.macromol.5b00439
*Macromolecules* 2015, 48, 2925–2934

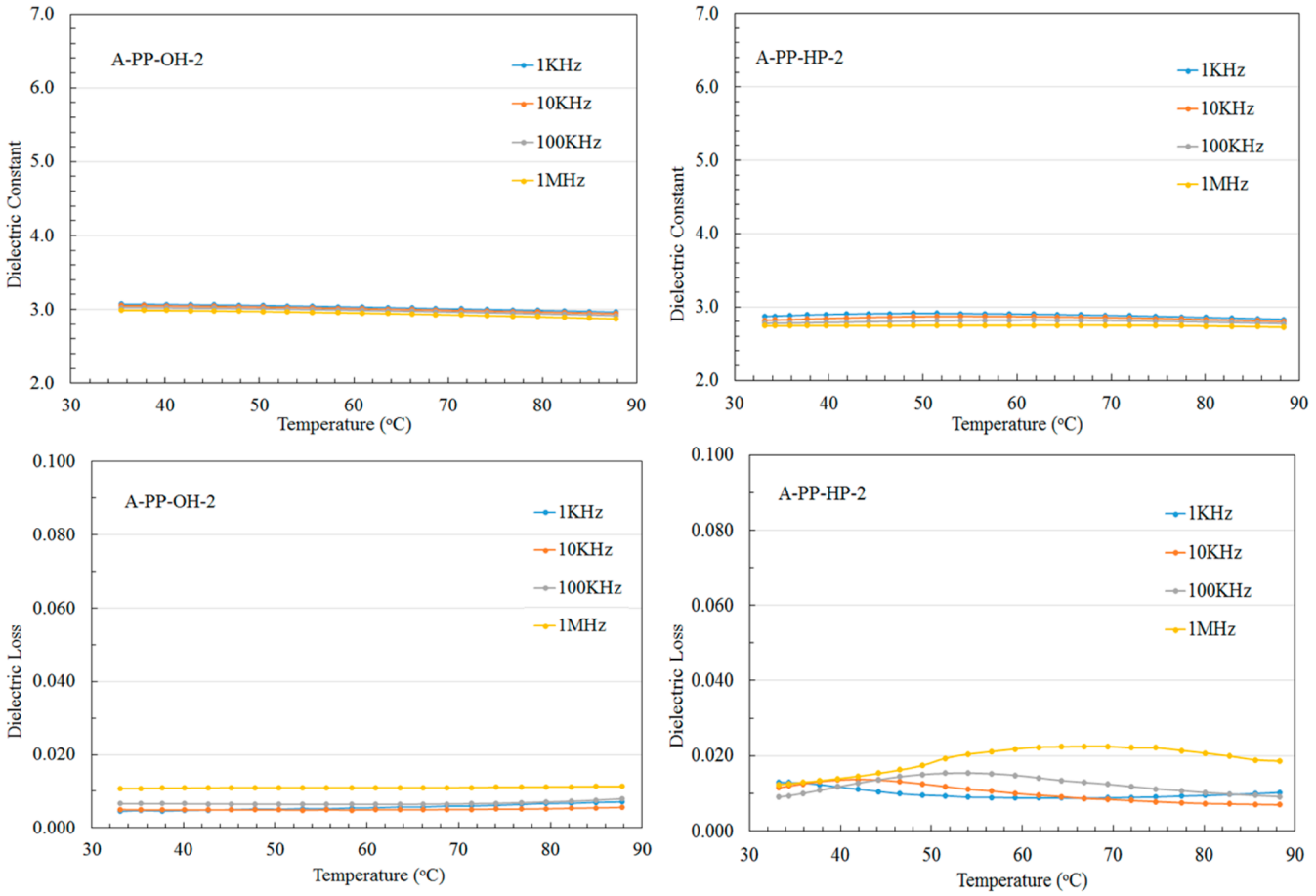


**Figure 8.** Dielectric constants and loss (vs frequency and temperature) for (left) A-PP-OH-2 and (right) A-PP-HP-2 tapered copolymers.

$CH_2$−OH chemical shift at 3.65 ppm in PP-OH sample completely disappeared with the appearance of two new chemical shifts in the PP-HP sample, including a triple chemical shift at 4.28 ppm for $CH_2$−O−C═O and a singlet chemical shift at 8 ppm for two aromatic protons in the hindered phenol moiety. Both chemical shifts also show a 1:1 peak intensity ratio. The combination clearly indicates the quantitative esterification reaction to obtain a highly pure PP-HP product. The same effective esterification reactions were also observed for all PP-OH samples using both hindered phenol molecules. Table 1 shows two sets of tapered and random PP-HP copolymers, prepared by PP-OH and 3,5-bis(*tert*-butyl)-4-hydroxybenzoic acid; they are used in this comparative study.

**Thermal Properties.** Figure 2 compares DSC curves between PP-HP with tapered and random microstructures and the corresponding PP-OH copolymers, respectively. In the tapered copolymer pair (A-PP-PH-2 and A-PP-OH-2), with long PP sequences and 1.7 mol % pendant HP or OH groups, the two DSC curves are nearly identical with the same melting temperature. Evidently, all the pendant functional groups are located in the amorphous domains, and the change of functional groups has no effect on the crystallization of long PP sequences. In the random copolymer case (B-PP-HP-3 and B-PP-OH-3), with short PP sequences and 4.7 mol % pendant HP or OH groups, there is only a small effect (~4 °C) on the melting temperature and crystallinity before and after the esterification reaction. The bulky HP groups with a relatively high concentration in the PP-HP copolymer may slightly slow down the crystallization kinetics. Overall, both $T_m$ and crystallinity seem to be primarily governed by branch density and are quite independent of side chain (comonomer) type, consistent with Flory's prediction[52,53] for semicrystalline copolymers. Under the equilibrium condition, each polymer chain runs from one side of lamellae to the other, and the consecutive propylene units govern the thickness of lamellae. The comonomer units with hindered phenol moieties are restricted in the amorphous regions.

Figure 3 shows two sets of DSC curves for the PP-HP copolymers (Table 1), which shall have similar DSC curves as their corresponding PP-OH copolymers. In set A, the tapered PP-HP copolymers (converted from the corresponding PP-OH copolymers prepared by heterogeneous Ziegler−Natta catalyst) show an initial reduction in both $T_m$ and $\Delta H$ values and then subsequently level off at the higher comonomer incorporation. Note that A-PP-HP-4 with 6.8 mol % HP content still shows a sharper melting endotherm with a high $T_m$ at 157 °C. Because of low comonomer reactivity for the 10-undecen-1-oxy-trimethylsilane comonomer in the heterogeneous Ziegler−Natta catalyst, the PP-OH intermediates and the final PP-HP copolymers have a "tapered" molecular structure, with the HP-containing side chain units concentrated at one end of the copolymer main chain. Therefore, the increase of comonomer content has less effect on the PP chain crystallization. On the other hand, in set B (the corresponding PP-OH copolymers prepared by the homogeneous metallocene catalyst) the comonomer incorporation systematically reduces PP crystallinity and crystal size. All melting temperature ($T_m$), heat of fusion ($\Delta H$), and crystallization temperature ($T_c$) decrease


DOI: 10.1021/acs.macromol.5b00439
*Macromolecules* 2015, 48, 2925−2934

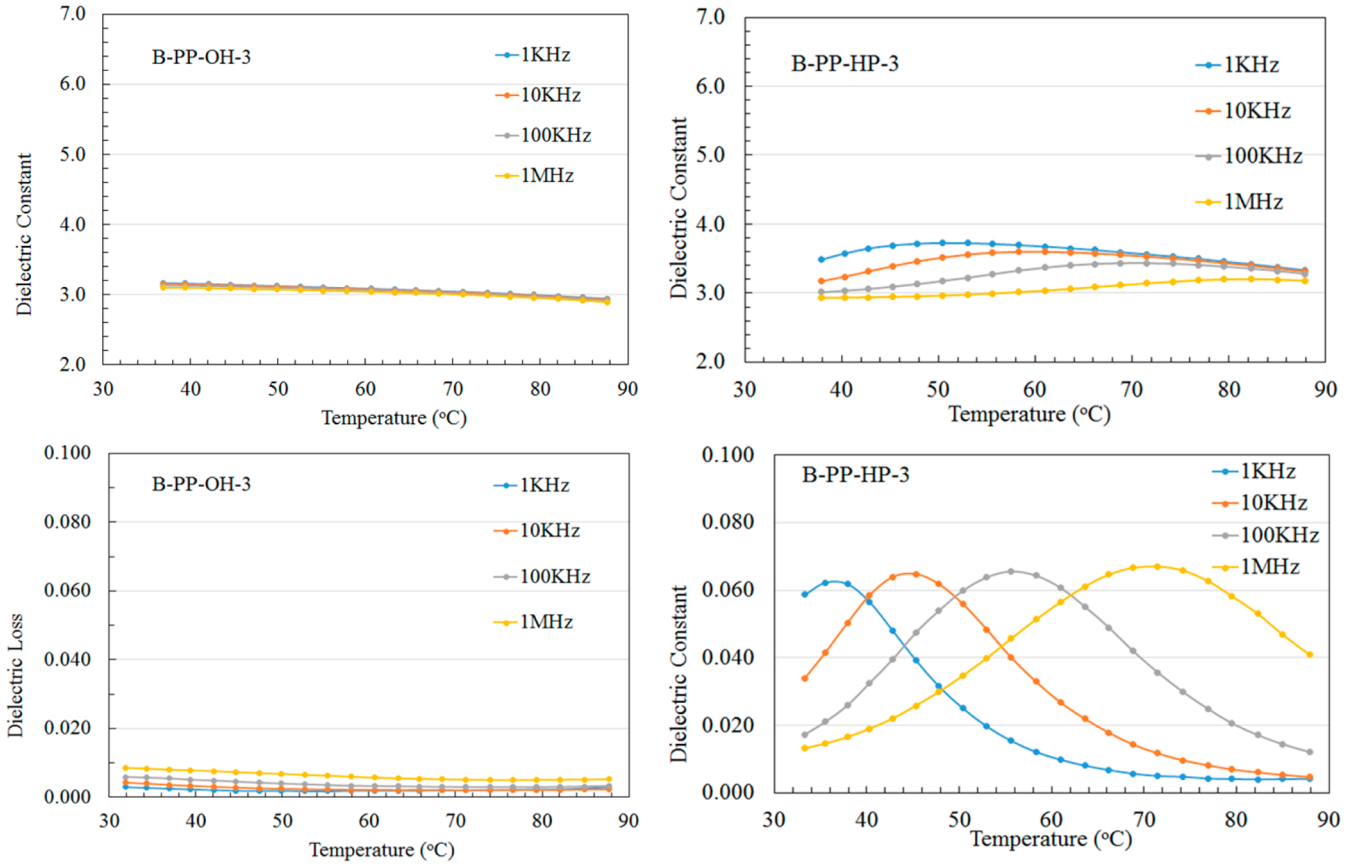


**Figure 9.** Dielectric constants and dielectric loss (vs frequency and temperature) for (left) B-PP-OH-3 and (right) B-PP-HP-3 random copolymers.

proportionally with the increase of the 1-decenol comonomer content. The B-PP-HP-4 copolymer, with 6 mol % comonomer content, nearly loses all crystallinity with a small melting peak $T_m$ at 82 °C. Evidently, the homogeneous *rac*-$Me_2Si$[2-Me-4-Ph(Ind)]$_2ZrCl_2$/MAO metallocene catalyst exhibits far more comparative comonomer reactivity ratios in forming a "random" copolymer microstructure.

It is interesting to understand the cocrystallization capability of PP-HP copolymers (stabilizers) with PP homopolymer and the difference between the two types of PP-HP copolymers with tapered and random microstructures. Figure 4 compares DSC curves of the first and second heating−cooling cycles for a physical mixture of PP-HP/PP powders using random and tapered PP-HP copolymers, respectively.

The experiment starts with a physical mixture of PP-HP and PP powders in an aluminum DSC sample pan with a cover and then heating the mixture to 200 °C (well beyond both melting temperatures) during the heating cycles. Upon heating, two molten polymer chains shall have chance to interdiffuse and cocrystallize into the same crystalline domain if possible, which can be observed in the subsequent cooling cycle with a single cocrystallization peak. In Figure 4 (top), the first heating cycle of the PP/A-PP-PH-2 (1/1) polymer blend shows a broad $T_m$ endotherm, with a main peak at 163 °C for PP and a small peak (shoulder) at 157 °C for tapered A-PP-OH-2 with 1.7 mol % OH content. In the following cooling cycle, there are two exothermic crystallization peaks at 115 and 130 °C, respectively, indicating two individual crystallization processes in forming PP-PH and PP crystalline domains. In the second heating cycle, the broad $T_m$ endotherm moves to a slightly lower temperature. To some extent, the PP/A-PP-PH-2 cocrystallization may also have occurred during the first cooling cycle. Keeping the molten state for slightly longer time to allow for interpolymer chain diffusion, there is only a single exothermic crystallization peak at 124 °C in the second cooling cycle, which is located between two crystallization peaks in the first cooling cycle. The combined DCS results clearly indicate the cocrystallization phenomenon between the tapered PP-HP copolymer and PP homopolymer. Because of high melting temperature and viscosity, the A-PP-OH-2 copolymer requires a long interchain diffusion time (without agitation) to mix with the PP homopolymer. On the other hand, Figure 4 (bottom) shows similar heating−cooling cycles between the PP homopolymer and the random B-PP-HP-3 copolymer with 4.7 mol % HP content. The two polymers have significantly different melting temperatures as shown in first heating cycle. However, a shape cocrystallization peak at 124 °C was observed during the cooling cycles as well as a single (but broad) melting peak in the subsequent heating cycles. The combination of low melting temperature and crystallinity in the B-PP-HP-3 copolymer may enhance its interchain diffusion and cocrystallization kinetics.

**Thermal Stability.** As discussed, the PP oxidative stability is a major concern during polymer processing and applications. The commercial PP products usually contain a small amount (<1 wt %) of hindered phenol stabilizers (Scheme 2) to prevent the thermal/oxidative polymer chain degradation. Figure 5 compares TGA curves of a pristine PP homopolymer under $N_2$ and air atmospheres. Without oxygen, PP shows its thermal stability up to >400 °C. It is clear the oxygen oxidation dominating PP chain degradation mechanism in air, which


DOI: 10.1021/acs.macromol.5b00439
*Macromolecules* 2015, 48, 2925−2934

begins its weight loss at about 210 °C, near its melt processing temperature.

It is very interesting to understand the performance of new PP-HP copolymers (PP-bonded hindered phenol stabilizers) and the comparison with regular hindered phenol stabilizers in air. Figure 6 compares TGA curves of a set of random PP-OH and PP-HP copolymers (with 4.7 mol % OH or HP content) with a pristine PP homopolymer and a commercial (dielectric grade) PP homopolymer with the IRGANOX1010 stabilizer at 10 °C/min heating rate under air atmosphere.

Compared with the pristine PP polymer that begins its weight loss at about 210 °C, the commercial PP product shows higher thermal stability with the initial weight loss temperature at 250 °C. On the other hand, the PP-HP copolymer shows significantly higher stability than both polymers with the initial weight loss temperature at 300 °C, about 50 and 90 °C higher than commercial PP and pristine PP, respectively. On the other hand, the starting PP-OH copolymer shows even lower initial weight loss temperature than the pristine PP, which may be associated with the vaporization of some tightly H-bonded $H_2O$ molecules. However, the PP-OH copolymer exhibits a slower weight loss profile. The comparison between the starting PP-OH and the corresponding PP-HP copolymers clearly demonstrates the effect of hindered phenol antioxidant moieties. Since the melt processing of PP usually operates between 200 and 220 °C, it is a common industrial practice to add some IRGANOX stabilizers in the PP products right after the polymerization. However, the stabilizers are consumed during the antioxidant protecting mechanism; it is important to provide a sufficient quantity of stabilizers in the PP matrix. Unfortunately, due to the polar nature of hindered phenol and the high mobility of small molecules, it is difficult to introduce a high concentration of IRGANOX stabilizers and maintain their uniform distribution in the polymer matrix.[54] These semicrystalline PP-HP copolymers, with high concentrations of polymer-bonded HP groups and a cocrystallization ability with the PP homopolymer, shall ensure adequate quantity and distribution of hindered phenol moieties presented during the PP melt processes and applications with long-term exposure to heat, UV radiation, and high applied electric field conditions.

Figure 7 (top) compares TGA curves of PP homopolymer and three B-PP-HP random copolymers (Table 1) with 1.5, 3.5, and 4.7 mol % of HP concentrations. The onset of polymer weight loss temperature is largely proportional to the concentration of HP groups; the higher the HP content, the higher the polymer stability. Note that the similarity of DSC profiles between B-PP-HP-1 with 1.5 mol % HP content and the dielectric-grade commercial PP polymer in Figure 6, which contains less than 1 wt % of the IRGANOX1010 stabilizer. Since each IRGANOX1010 molecule has four hindered phenol groups (Scheme 2), two PP materials shall have similar HP contents. Figure 7 (bottom) shows the TGA curves of B-PP-HP-3/PP blends by mixing a random PP-HP copolymer with 4.7 mol % HP content and PP homopolymer with various weight ratios, respectively. The dilution of the HP concentration in the PP matrix by polymer blending also shows a systematic reduction of thermal-oxidative stability. Similar experimental results were also observed in the tapered PP-HP copolymer system with the thermal/oxidative stability controlled by HP content. The TGA curves of A-PP-HP/PP blends are also located between two individual A-PP-HP and PP curves and higher PP-HP content higher thermal stability. Overall, both random and tapered PP-HP copolymers are effective stabilizers with a somewhat small difference in their performance. As expected in the semicrystalline morphology, all pendant HP moieties in both tapered and random PP-HP copolymers are located in amorphous phases that are most vulnerable to the oxygen diffusion and oxidation. The PP-HP copolymer (i.e., a polymer-bonded stabilizer that shows cocrystallization with the PP homopolymer) can provide a high concentration of hindered phenol (polar) moieties in the PP (nonpolar) matrix without forming phase separation and the homogeneous distribution of these HP antioxidants in PP amorphous phases. This combination shall also be beneficial by offering long-term thermal-oxidative protection of the PP products under various application conditions.

**Dielectric Properties.** One of our major research objectives is to develop new functional PP polymers that can exhibit better dielectric properties with high effective energy storage capacity, as well as long-term stability under a high temperature and high applied electric field conditions. Figure 8 compares dielectric profiles of the same pair of tapered A-PP-OH-2 and A-PP-HP-2 copolymers (with 1.7 mol % comonomer content), over a wide range of temperatures (from −20 to 80 °C) and frequencies (1 kHz to 1 MHz). They show a dielectric constant of $\varepsilon$ = 3 and 2.8, respectively, both significantly higher than the PP polymer ($\varepsilon$ = 2.2). As shown in the Supporting Information (Figure S2), the dielectric constant systematically increases with the increase of polar OH and HP functional groups, and the dielectric loss maintains relatively low. However, in the side-by-side comparison, the PP-HP copolymer consistently shows a slightly lower dielectric constant and higher dielectric loss than the corresponding PP-OH copolymer, despite the fact that the hindered phenol moiety contains both a polar OH group and polarizable $\pi$-electrons. Evidently, two bulky *tert*-butyl groups surrounding the OH moiety in the hindered phenol moiety may block the formation of H-bonding between OH groups and their association with water molecules under normal sample handling conditions. As discussed in our previous papers, the primary OH groups in PP-OH copolymer are capable of forming strong H-bonding between pendant OH groups and absorbing some external $H_2O$ molecules.[55,56] The associated $H_2O$ molecules contribute to the overall dielectric constant in PP-OH. On the other hand, all PP-HP copolymers (Figure 7) show flat TGA base lines (without weight loss up to 200 °C), indicating no $H_2O$ molecules associated with the PP-HP copolymers. Furthermore, the loss of H-bonding between pendant OH groups in the amorphous phase reduces PP-HP polarization reversibility. The slow polarization−depolarization kinetics are clearly reflected in the larger dielectric loss and the frequency-dependent loss profile.

Figure 9 compares the dielectric profiles between the random B-PP-OH-3 copolymer with 4.7 mol % OH content and its corresponding B-PP-HP-3 copolymer over a range of frequencies (between 1 kHz and 1 MHz) and temperatures (between 30 and 90 °C). In this copolymer pair, they show quite different dielectric constant and loss profiles (vs temperature and frequency). In the B-PP-OH-3 copolymer, the dielectric constant ($\varepsilon$ = 3.3) and dielectric loss (tan $\delta$ < 0.01) are almost constant over the entire temperature and frequency ranges, but the corresponding B-PP-HP-3 film shows much stronger frequency and temperature dependence. With the increase of frequency, the loss intensity systematically increases and the loss peak also shifts to higher temperature. Similar results were also observed in other random PP-HP



DOI: 10.1021/acs.macromol.5b00439
*Macromolecules* 2015, 48, 2925−2934

copolymers (shown in Figures S3 and S4 in the Supporting Information). A clear phase transition in the random PP-HP copolymers begins at about 35−50 °C at 1 kHz, with both dielectric constant and loss peaks shifting to higher temperature with higher frequency, which may be associated with side chain motion in the amorphous phase under the applied electric field. The combined reduction of crystallinity, melting temperature, and H-bonding diminishes the polarization reversibility of the pendant polar groups in the time scale of the polarization process.

Overall, both tapered and random PP-OH dielectric profiles generally resemble the PP profile, with a dielectric constant ($\varepsilon$) that is independent over the range of frequencies and temperatures, and the dielectric loss maintains relatively low. The hydrogen bonding between OH side chains in the amorphous phase provides the secondary interactive force between polymer chains and reversible polarization, which may also contribute to the low loss under the applied electric fields. On the other hand, the corresponding PP-HP copolymers (without H-bonding) show much larger dielectric profile difference between tapered and random microstructures. In the tapered PP-HP structure, the combination of high crystallinity and high melting temperature in the strong crystalline domains may minimize the segmental motion in the amorphous phase.

## CONCLUSION

This paper discusses a new class of polypropylene-based stabilizers (PP-HP copolymers) containing a PP backbone and various concentrations of hindered phenol (antioxidant) moieties that are located in the pendant side chains. An effective synthesis route has been developed to prepare these semicrystalline PP-HP copolymers with well-controlled microstructures, including tapered and random copolymers. Evidently, these PP-HP polymeric stabilizers with both tapered and random microstructures show the cocrystallization phenomenon with the PP homopolymer, which provides an ideal mechanism for introducing a high concentration of HP antioxidants that are homogeneously distributed and immobilized in the PP amorphous matrix. The combination provides PP-HP copolymers and their PP-HP/PP blends with exceptionally high thermal-oxidative stability that is tunable by the incorporated HP content. This new antioxidant mechanism may be particularly beneficial in the long-term protection of PP products under severe application conditions, which is currently under investigation. Those experimental results will be reported in the near future. A systematic study has also been conducted to find the most suitable PP-HP copolymer for dielectric and capacitor applications, which offer the PP dielectric thin films, with not only better stability but also a higher dielectric performance (high dielectric constant and low loss). The tapered PP-HP copolymer with high crystallinity and high melting temperature is found to be the most suitable microstructure.

## ASSOCIATED CONTENT

### Supporting Information

Synthesis of 10-undecen-1-oxytrimethylsilane monomer, copolymerization of propylene/10-undecen-1-oxytrimethylsilane by $TiCl_3$·AA/$Al(Et)_2Cl$ and *rac*-$Me_2Si$[2-Me-4-Ph-(Ind)]$_2ZrCl_2$/MAO catalysts, preparation of dielectric films, $^1$H NMR spectrum of 10-undecen-1-oxytrimethylsilane, and dielectric constant and loss of several PP-OH and PP-HP copolymers. The Supporting Information is available free of charge on the ACS Publications website at DOI: 10.1021/acs.macromol.5b00439.

## AUTHOR INFORMATION

### Corresponding Author

*E-mail chung@ems.psu.edu (T.C.M.C.).

### Notes

The authors declare no competing financial interest.

## ACKNOWLEDGMENTS

The authors gratefully acknowledge the financial support of this work through a Multidisciplinary University Research Initiative (MURI) grant from the Office of Naval Research under Contract N00014-10-1-0944.

## REFERENCES

(1) Emanuel, N. M.; Buchachenco, L. M. *Chemical Physics of Polymer Degradation and Stabilization*; VNU Science Press: Zeist, Netherlands, 1987.
(2) Al-Malika, S. Effects of Antioxidants and Stabilization. In *Comprehensive Polymer Science*; Allen, G., Bevington, J. C., Eds.; Pergamon Press: New York, 1989; Vol. *6*, p 539.
(3) *Degradation and Stabilization of Polyolefins*; Allen, N. S., Ed.; Applied Science Publishers: London, 1983; 384 pp.
(4) *Polymer Durability*; Clough, R., Billingham, N. C., Gillen, K. T., Eds.; Advances in Chemistry Series 249; American Chemical Society: Washington, DC, 1996; 712 pp.
(5) Lutz, Jr., J. T. *Thermoplastic Polymer Additives. Theory and Practice*; Marcel Dekker: New York, 1989.
(6) Gugumus, F. *Plastics Additives*, 3rd ed.; Oxford University Press: New York, 1990.
(7) Ammala, A.; Bateman, S.; Dean, K.; Petinakis, E.; Sangwan, P.; Wong, S.; Yuan, Q.; Yu, L.; Patrick, C.; Leong, K. H. *Prog. Polym. Sci.* **2011**, *36*, 1015.
(8) Kolbert, A. C.; Joseph, G. D.; Xu, L. S. *Macromolecules* **1996**, *29*, 8591.
(9) Mowery, D. M.; Clough, R. L.; Assink, R. A. *Macromolecules* **2007**, *40*, 3615.
(10) Mowery, D. M.; Assink, R. A.; Derzon, D. K.; Klamo, S. B.; Clough, R. L.; Bernstein, R. *Macromolecules* **2005**, *38*, 5035.
(11) Tobolsky, A. V.; Norling, P. M.; Frick, N. H.; Yu, H. *J. Am. Chem. Soc.* **1964**, *86*, 3925.
(12) Scheirs, J.; Pospíšil, J.; O'Connor, M. J.; Bigger, S. W. *Polymer Durability*; Chapter 24, pp 359−374 2009.
(13) Stillson, G. H.; Sawyer, D. W.; Hunt, C. K. *J. Am. Chem. Soc.* **1945**, *67*, 303.
(14) Cook, C. D.; Woodworth, R. C. *J. Am. Chem. Soc.* **1953**, *75*, 6242.
(15) Dopico-García, M. S.; López-Vilariño, J. M.; González-Rodríguez, M. V. *J. Agric. Food Chem.* **2007**, *55*, 3225.
(16) Stagnaro, P.; Mancini, G.; Piccinini, A.; Losio, S.; Sacchi, M. C.; Viglianisi, C.; Menichetti, S.; Adobati, A.; Limbo, S. *J. Polym. Sci., Part B: Polym. Phys.* **2013**, *51*, 1007.
(17) *Antioxidant Polymers*; Cirillo, G., Iemma, F., Eds.; Wiley: Hoboken, NJ, 2012.
(18) Wilén, C. E.; Auer, M.; Strandén, J.; Näsman, J. H.; Rotzinger, B.; Steinmann, A.; King, R. E.; Zweifel, H.; Drewes, R. *Macromolecules* **2000**, *33*, 5011.
(19) Menichetti, S.; Viglianisi, C.; Liguori, F.; Cogliati, C.; Boragno, L.; Stagnaro, P.; Losio, S.; Sacchi, M. C. *J. Polym. Sci., Part A: Polym. Chem.* **2008**, *46*, 6393.
(20) Wu, W. J.; Zeng, X. R.; Li, H. Q.; Lai, X. J.; Li, F.; Guo, J. H. *J. Macromol. Sci., Part B: Phys.* **2014**, *53*, 1244.
(21) Wilén, C. E.; Näsman, J. H. *Macromolecules* **1994**, *27*, 4051.


DOI: 10.1021/acs.macromol.5b00439
*Macromolecules* 2015, 48, 2925−2934

(22) Wilén, C. E.; Luttikhedde, H.; Hjertberg, T.; Näsman, J. H. *Macromolecules* **1996**, *29*, 8569.
(23) Auer, M.; Nicolas, R.; Rosling, A.; Wilén, C. E. *Macromolecules* **2003**, *36*, 8346.
(24) Kim, T. H.; Kim, H. K.; Oh, D. R.; Lee, M. S.; Chae, K. H.; Kaang, S. *J. Appl. Polym. Sci.* **2000**, *77*, 2968.
(25) Munteanu, D.; Csunderlik, C. *Polym. Degrad. Stab.* **1991**, *34*, 295.
(26) Dolatkhani, M.; Cramail, H.; Deffieux, A.; Santos, J. M.; Ribeiro, M. R.; Bordado, J. M. *Macromol. Chem. Phys.* **2003**, *204*, 1889.
(27) Zhang, Y. J.; Li, H. Y.; Zhang, Y.; Li, Q.; Ma, Z.; Dong, J. Y.; Hu, Y. L. *Macromol. Chem. Phys.* **2014**, *215*, 763.
(28) Kim, T. H.; Oh, D. R. *Polym. Degrad. Stab.* **2004**, *84*, 499.
(29) Kim, T. H. *J. Appl. Polym. Sci.* **2004**, *94*, 2117.
(30) Chung, T. C. *Functionalization of Polyolefins*; Academic Press: London, 2002.
(31) Nash, J. L. *Polym. Eng. Sci.* **1988**, *28*, 862.
(32) Michalczyk, P.; Bramoulle, M. *IEEE Trans. Magn.* **2003**, *39*, 362.
(33) Banford, H. M.; Fouracre, R. A.; Faucitano, A.; Buttafava, A.; Martinotti, F. *IEEE Trans. Dielectr. Electr. Insul.* **1996**, *3*, 594.
(34) Reed, C. W.; Cichanowski, S. W. *IEEE Trans. Dielectr. Electr. Insul.* **1994**, *1*, 904.
(35) Sarjeant, W. J.; MacDougall, F. W.; Larson, D. W. *IEEE Electr. Insul. Mag.* **1997**, *13*, 20.
(36) Picci, G.; Rabuffi, M. *IEEE Trans. Plasma Sci.* **2000**, *28*, 1603.
(37) Chung, T. C. *Macromolecules* **2013**, *46*, 6671.
(38) Chung, T. C. *Adv. Polym. Sci.* **2013**, *258*, 233.
(39) Zhang, M.; Colby, R. H.; Milner, S. T.; Chung, T. C.; Huang, T. Z.; deGroot, W. *Macromolecules* **2013**, *46*, 4313.
(40) Zhang, M.; Yuan, X. P.; Wang, L.; Chung, T. C.; Huang, T. Z.; deGroot, W. *Macromolecules* **2014**, *47*, 571.
(41) Lin, W. T.; Shao, Z.; Dong, J. Y.; Chung, T. C. *Macromolecules* **2009**, *42*, 3750.
(42) Langston, J. A.; Colby, R. H.; Chung, T. C.; Shimizu, F.; Suzuki, T.; Aoki, M. *Macromolecules* **2007**, *40*, 2712.
(43) Yuan, X.; Chung, T. C. *Appl. Phys. Lett.* **2011**, *98*, 62901.
(44) Misra, M.; Agarwal, M.; Sinkovits, D. W.; Kumar, S.; Wang, C.; Pilania, G.; Ramprasad, R.; Weiss, R. A.; Yuan, X.; Chung, T. C. *Macromolecules* **2014**, *47*, 1122.
(45) Spaleck, W.; Kueber, F.; Winter, A.; Rohrmann, J.; Bachmann, B.; Antberg, M.; Dolle, V.; Paulus, E. F. *Organometallics* **1994**, *13*, 954.
(46) Brandrup, J.; Immergut, E. H. *Polymer Handbook*, 3rd ed.; Wiley Interscience: New York, 1989; p VII-7.
(47) Chung, T. C. *Prog. Polym. Sci.* **2002**, *27*, 39.
(48) Neises, B.; Steglich, W. *Angew. Chem., Int. Ed.* **1978**, *17*, 522.
(49) Chung, T. C.; Rhubright, D. *Macromolecules* **1993**, *26*, 3019.
(50) Yuan, X. P.; Matsuyama, Y.; Chung, T. C. *Macromolecules* **2010**, *43*, 4011.
(51) Chung, T. C. *Green Sustainable Chem.* **2012**, *2*, 29.
(52) Flory, P. J. *Trans. Faraday Soc.* **1955**, *51*, 848.
(53) Flory, P. J. *J. Chem. Phys.* **1949**, *17*, 223.
(54) Pospíšil, J.; Habicher, W. D.; rek, S. N. *Macromol. Symp.* **2001**, *164*, 389.
(55) Wang, C. C.; Pilania, G.; Ramprasad, R.; Agarwal, M.; Misra, M.; Kumar, S.; Yuan, X. P.; Chung, T. C. *Appl. Phys. Lett.* **2013**, *102*, 152901.
(56) Gupta, S.; Yuan, X. P.; Chung, T. C.; Kumar, S.; Cakmak, M.; Weiss, R. A. *Macromolecules* **2013**, *46*, 5455.


DOI: 10.1021/acs.macromol.5b00439
*Macromolecules* 2015, 48, 2925−2934